Structural Behavior of Barges in High-Energy Collisions against Bridge Piers

Francisco J. Luperi, Ph.D.[1] and Federico Pinto, Ph.D.[2]

Abstract: The collision of barges against bridge piers is an extreme loading condition that usually governs the design of bridges that span navigable waterways. The magnitude and time variation of impact forces depend on several aspects, such as mass and speed of barges, stiffness of impacted structure, and structural behavior of the barge. The latter has a considerable influence, not only because it defines the maximum possible impact force but also because it defines the energy absorption capacity of the barge. The structural behavior of barges has been studied using scale models and numerical methods. However, the total deformation reached in these studies was limited to the size of the barge bow. Hence, there is uncertainty in the behavior for high-energy collisions, where deformations may well exceed this deformation range. This paper studies the structural behavior of barges using detailed nonlinear finite-element (FE) models. Load-deformation relationships are established on the basis of the model results for different shapes and sizes of impacted structures. These relationships can be applied in simplified dynamic analyses for design, considering the large deformations expected for high-energy impact scenarios. Simplified analysis methods for symmetric and oblique flotilla impacts are presented and validated against full FE. **DOI: 10.1061/(ASCE)BE.1943-5592.0000789.**

Author keywords: Bridge; Barge; Structure; Collision; Impact.

Introduction

The structural behavior of barges has a significant influence on the analysis of barge collisions against bridge piers or protection structures. The impact-force history during barge–bridge collisions depends on several factors, such as mass and speed of barges, stiffness of the impacted structure, and the configuration of barge flotilla. The structural behavior of the impacting barge defines the maximum impact force developed during collision, as well as the energy absorption capacity of the barge. The structural behavior of European Type II and Type IIa barges was studied using scale physical models (Meier-Dörnberg 1983), whereas the behavior of Jumbo hopper and oversize tanker barges was studied using high-resolution finite-element (FE) models (Harik et al. 2008; Consolazio et al. 2008, 2010a). The main goal of these studies was to define the load-deformation behavior of the barge bow through simplified force-deformation relationships for the development of simplified design procedures. However, the maximum deformation considered by these authors is less than the length of the barge bow, which renders these load-deformation curves applicable to a limited range of energy. Hence, there is uncertainty in the structural behavior of barges for high-energy collisions, where the energy absorbed by the barge may lead to deformations exceeding the range considered by these previous studies. This paper focuses on the behavior of barges for a deformation range larger than that used in previously published studies and proposes analysis methods to account for the forces developed in this deformation range. Simplified methods applicable for high-energy collisions are proposed and validated using detailed FE models.

Scale Physical Models

The guidelines developed by the European Committee for Standardization (CEN 1991) and AASHTO (2012) provide simplified design methods considering a force-deformation relationship obtained by Meier-Dörnberg (1983) on the basis of scale physical models. The force-deformation relationships obtained by Meier-Dörnberg are bilinear and represent mean and upper bound values of the test results (Fig. 1).

The CEN (1991) adopts the mean curve and provides a simplified procedure to estimate a time history of impact forces on the basis of the kinetic energy of the barge. AASHTO (2012), on the other hand, recommends a static impact force, also obtained as a function of the kinetic energy of the barge. The equivalent *static force* concept proposed by AASHTO (2012) has been criticized in the recent literature (e.g., Consolazio et al. 2008; Harik et al. 2008).

The bilinear force-deformation relationships considered by AASHTO and CEN consider a steady increase in load after yielding (Fig. 1). Recent research, however, indicates that the yield load actually remains approximately constant or even decreases with increasing deformations (Consolazio et al. 2008; Harik et al. 2008).

Numerical Models

The structural behavior of Jumbo hopper and oversize tanker barges was studied using high-resolutionFE models by Consolazio et al. (2008) and Harik et al. (2008). These authors considered the influence of different pier shapes and sizes; factors that were found to have a significant influence on the resulting forces. Consolazio

[1]Profesor Asistente, Dep. Estructuras F.C.E.F.yN., Univ. Nacional de Córdoba – CONICET, Casilla de Correo 916, Córdoba, Argentina. E-mail: fluperi@efn.uncor.edu

[2]Profesor Asociado. Dep. Estructuras F.C.E.F.yN., Univ. Nacional de Córdoba – CONICET, Casilla de Correo 916, Córdoba, Argentina (corresponding author). E-mail: fpinto@efn.uncor.edu

Note. This manuscript was submitted on August 29, 2014; approved on February 27, 2015; published online on [redacted]. Discussion period open until [redacted]; separate discussions must be submitted for individual papers. This paper is part of the ***Journal of Bridge Engineering***, © ASCE, ISSN 1084-0702/040[redacted](14)/$25.00.

et al. (2008) describe that there is a decrease in contact force associated with the buckling process of the internal reinforcements and failure of the hull. These authors also found that the contact force increases with the size of the impacted pier.

Harik et al. (2008) indicate that barge–bridge collisions are not high-speed impact events because the results obtained using dynamic and pseudostatic analyses are very similar. Hence, velocity does not significantly influence the crushing resistance of the barge, with the exception of a sharp peak force developed at the beginning of the impact process. Harik et al. (2008) report that this initial peak force is too brief to significantly affect typical bridge structures. Typical force-deformation curves derived by Consolazio et al. (2008) and Harik et al. (2008) for Jumbo hopper barges are shown in Figs. 2 and 3, respectively. On the basis of these results, simplified force-deformation relations are proposed by these authors for developing improved simplified analysis techniques. Consolazio et al. (2008) propose an elastic-perfectly plastic behavior, whereas Harik et al. (2008) derive piecewise linear relationships.

Consolazio et al. (2010a, b) propose several simplified analysis techniques, including a static analysis method (static bracketed impact analysis), a predefined load-history method [applied vessel impact loading (AVIL)], a response spectrum method (impact response spectrum analysis), and a barge–structure interaction approach [coupled vessel impact analysis (CVIA)]. Harik et al. (2008) propose a series of FEM regressions that allow the definition of impact load and collision duration, as well as a spring–mass model for barge flotillas.

These design methods are, however, based on force-deformation relationships only valid for a limited deformation range (less

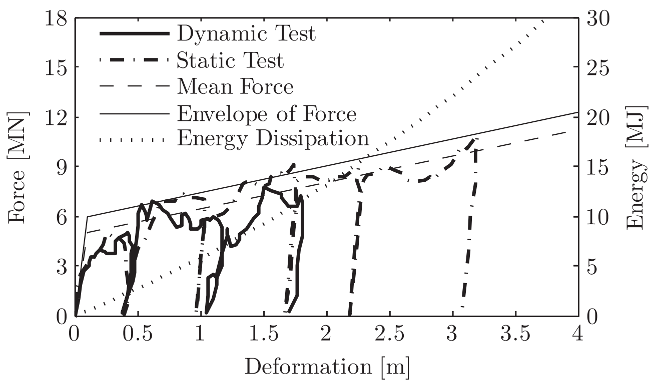

6 **Fig. 1.** Load deformation curves for European barges Type II and Type IIa

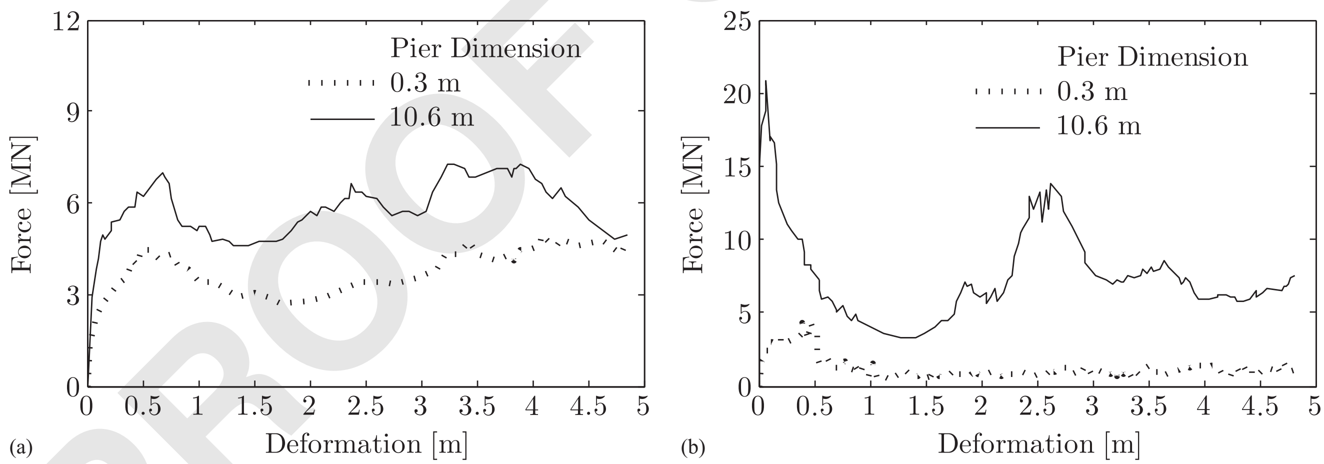

Fig. 2. Impact force versus deformation for Jumbo hopper obtained using numerical model of barge bow for (a) round piers; and (b) flat piers (data from Consolazio et al. 2008)

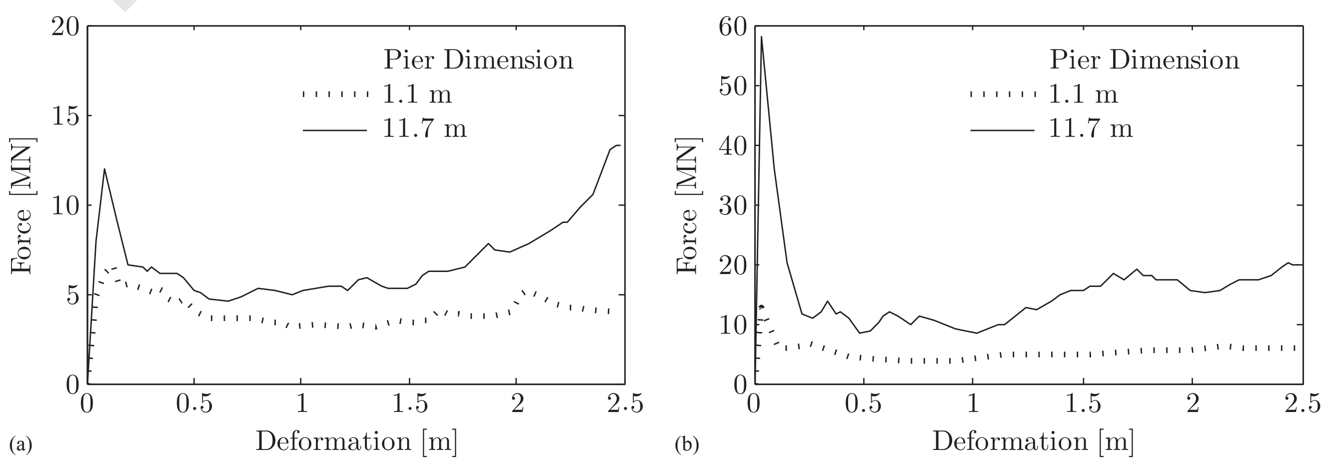

Fig 3. Impact force versus deformation for Jumbo hopper obtained using numerical model of barge bow for (a) round piers; and (b) flat piers (data from Harik et al. 2008)

than the length of the barge bow). There are design situations where the kinetic energy involved leads to bow deformations that exceed the range considered by these authors. For example, considering that average barge tows consist of 15 barges but may go up to 40 barges (e.g., CARIA 2014), and that each barge may have a displacement of 1,900 t (e.g., AASHTO 2012), the kinetic energy involved may be on the order of 360 MJ (or more) for a velocity of 5 m/s (e.g., Pinto et al. 2008). Even considering that the flotilla may break upon impact, the kinetic energy of a single column of five barges at 5 m/s yields 120 MJ. Considering a kinetic energy of 120 MJ, and the force-deformation relationship recommended by AASHTO (2012), the permanent barge deformation would yield 9.5 m, largely exceeding the deformation range considered by previous studies.

Structural Behavior of Barge

The structural behavior of Parana cargo and tanker barges is investigated using nonlinear FE models, on the basis of structural drawings and specifications provided by a regional barge manufacturer. Table 1 shows a comparison of the main features of the Parana, Jumbo hopper, and oversize tanker barges, where it is seen that the Parana cargo is similar to the Jumbo hopper, but provides a greater displacement capacity.

The main purpose of the FE analyses is to extend the force-deformation relationship up to 14 m of bow deformation to assess previously proposed trends (i.e., elastic-perfectly plastic or constant hardening) for this deformation range.

Barge Structure

The Parana cargo and tanker barges are 59.5 m long, with a loaded displacement of 3,100 and 2,900 t, respectively (Table 1). The hulls of these barges are double, and consist of A36 steel plates with L-shaped stiffeners 7.93–19 mm in thickness. These structures include longitudinal and transverse reinforcing sections consisting of L-shaped and U-shaped internal trusses, as well as watertight sections.

Table 1. Typical Barge Characteristics

Parameters	Jumbo hopper	Oversize tanker	Parana type: Cargo	Parana type: Tanker
Length (m)	59.3	88.2	59.5	59.5
Width (m)	10.7	16.1	16	16
Depth of vessel (m)	3.6	3.6	3.6	3.6
Loaded displacement (t)	1,900	4,300	3,100	2,900

Fig. 4 shows the geometry of tanker and cargo barges, including partial views of the reinforcing and watertight sections. The ASTM A36 stress–strain relationship considered in the FE models is shown in Fig. 5 (Boyer 2002).

Finite-Element Models

The structural behavior of the barges was modeled using SIMULIA (2010). The hull and internal trusses (SR3 and SR4) were modeled using shell elements with reduced integration, an assumed shear deformation for bending, and hourglass control for membrane behavior. Geometric nonlinearities were also taken into account. Following Harik et al. (2008), a strain rate–independent material definition is considered, as these authors found that strain rate effects are negligible for these types of problems. The payload was not explicitly modeled, but its inertia was accounted for using an additional mass distributed in the barge body. The welded unions between hull sheets and between the hull and internal trusses were modeled using constraints. Hence, the possibility of weld rupture is not accounted for in the model. However, failure of the steel was considered for an equivalent plastic deformation of 20% by eliminating the elements reaching this threshold.

The impacted structure was modeled as a rigid object to evaluate the load-deformation relationship of the barges. However, the dynamic behavior of the impacted structure can be accounted for in subsequent analysis. A general contact algorithm, able to detect contacts among different parts of the model, is considered. An explicit dynamic scheme was preferred over an implicit analysis because of the large number of contacts expected. The lashings between barges were defined as tension only, elastic-

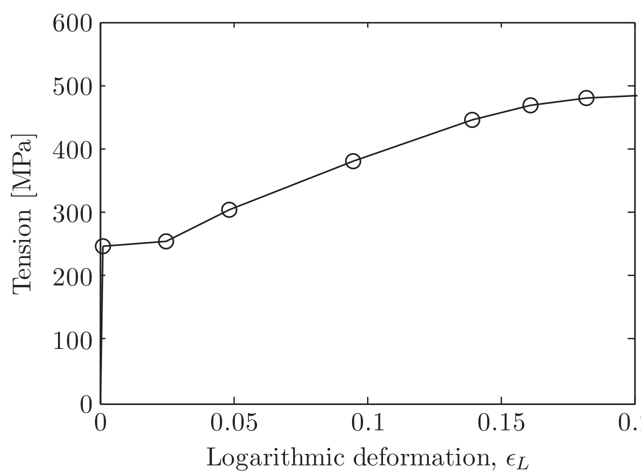

Fig. 5. Stress–strain relationship of ASTM A36 steel

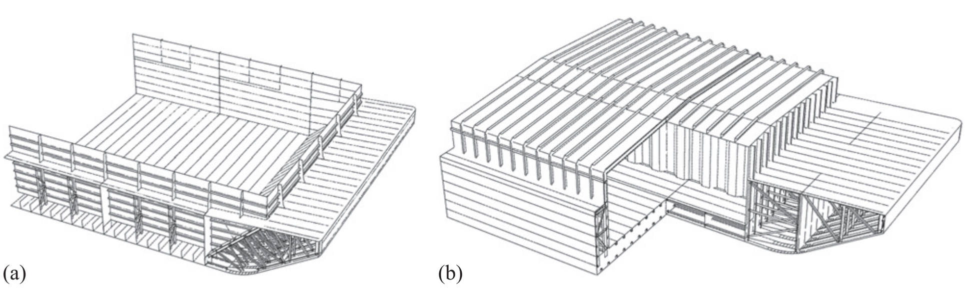

Fig 4. Geometry of Parana cargo and tanker barges

perfectly plastic elements, with failure due to excessive straining. The lashing models considered herein follow the properties and usual practices described by Arroyo and Ebeling (2005).

To limit the complexity of the model, hydrodynamic effects were not taken into account. However, hydrodynamic effects can be included in the analysis using a hydrodynamic mass coefficient, as proposed by AASHTO (2012).

Force-deformation relationships for barges were obtained by performing several collision simulations. The analyses considered centered and corner impacts against flat and round piers. Oblique collisions against flat walls with different impact angles were also analyzed.

The FE models were set up following two different approaches for the geometry: (1) the partial-barge model and (2) the full-barge model.

These two different approaches have been considered by other researchers for the analysis of the structural response of barges (Consolazio et al. 2008; Harik et al. 2008). In the first approach, only the front portion of the barge (about 20 m out of a total length of 60 m) was modeled. A boundary condition consisting of a constant velocity was imposed in this approach. A uniform mesh was considered because the deformation develops throughout a significant part of the model [Fig. 6(a)].

In the second approach, the complete barge was represented, and an initial velocity condition was defined. In this model, the hydrostatic behavior of water was represented using linear springs applied at the bottom of the entire barge along a direction perpendicular to this surface. In this approach, a graded mesh was defined because deformation concentrates in the front portion of the model [Fig. 6(b)].

To isolate the influence of the boundary conditions in the model results, both approaches consider the same mesh size in the barge bow. Fig. 7 shows a comparison of the force-deformation relationships obtained using both approaches. It can be seen that the partial-barge model yields higher forces at the beginning of the deformation process (mainly crushing near the bow), for both cargo and tanker barge types. There are also some differences in forces for greater deformations, where forces obtained using the partial model are similar or less than the values obtained using the full-barge model. The force-deformation relationships reported by Consolazio et al. (2010a) consider a partial-barge model.

Results presented in the following sections consider the full-barge model results, as they are deemed more representative of actual barge behavior.

Results

The following general trends are identified in the different FE model simulations (Figs. 9–12):

- The magnitude of contact forces depends on pier shape and size. In general terms, the mean force increases with pier width and is greater for flat piers versus rounded piers. These trends are also reported by Consolazio et al. (2010a) on the basis of partial-barge models.
- An initial peak force is observed, which corresponds to a deformation on the order of 0.05–0.1 m. The deformation corresponding to this initial peak is limited to the zone adjacent to the pier [Fig. 8(a)]. This peak force is higher for flat piers (Figs. 9 and 10).

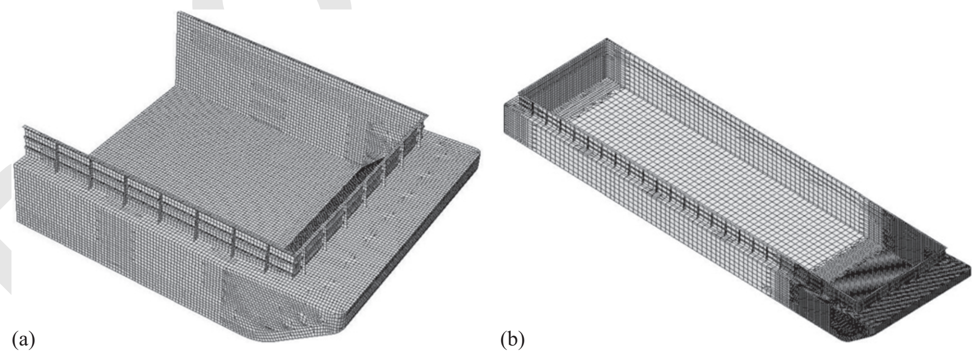

Fig. 6. Partial-barge and full-barge models

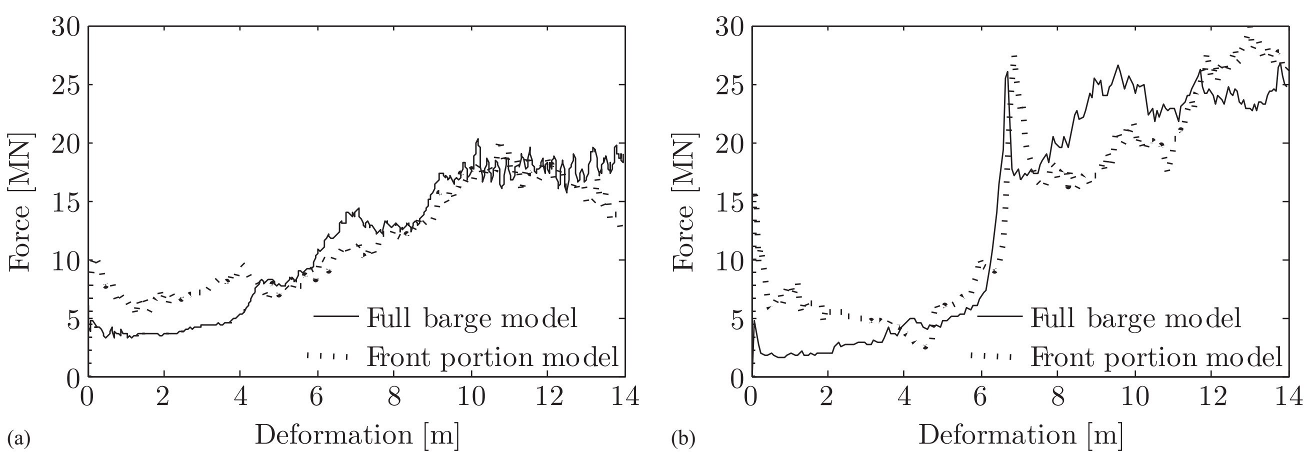

Fig. 7. Finite-element results for partial-barge and full-barge models: (a) cargo barge against 10 m round pier; (b) tanker barge against 6 m flat pier

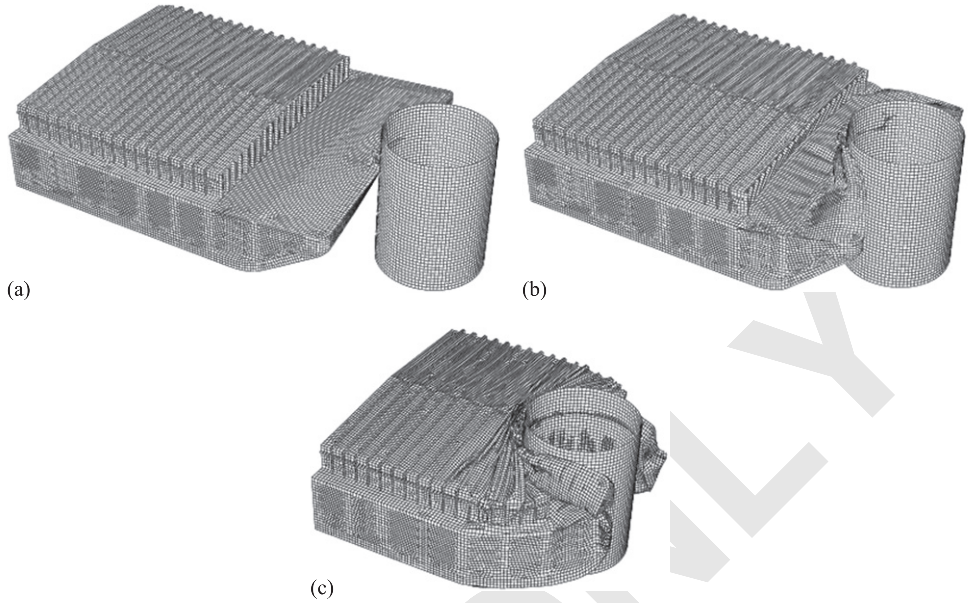

Fig. 8. Deformation of tanker barge impacting a round pier

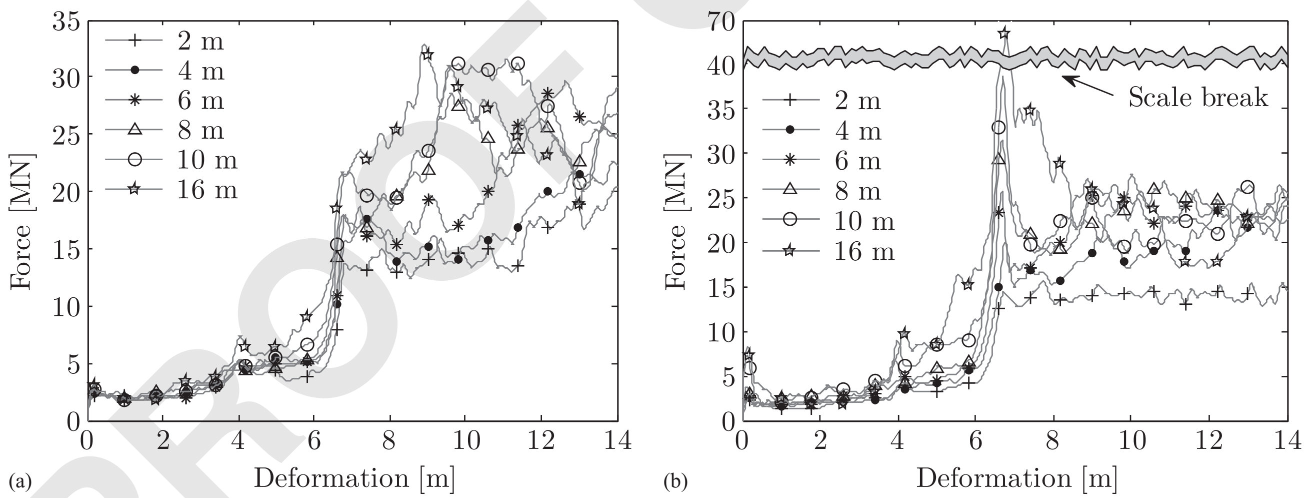

Fig. 9. Load deformation for tanker barge for centered impact against (a) round pier; and (b) flat pier

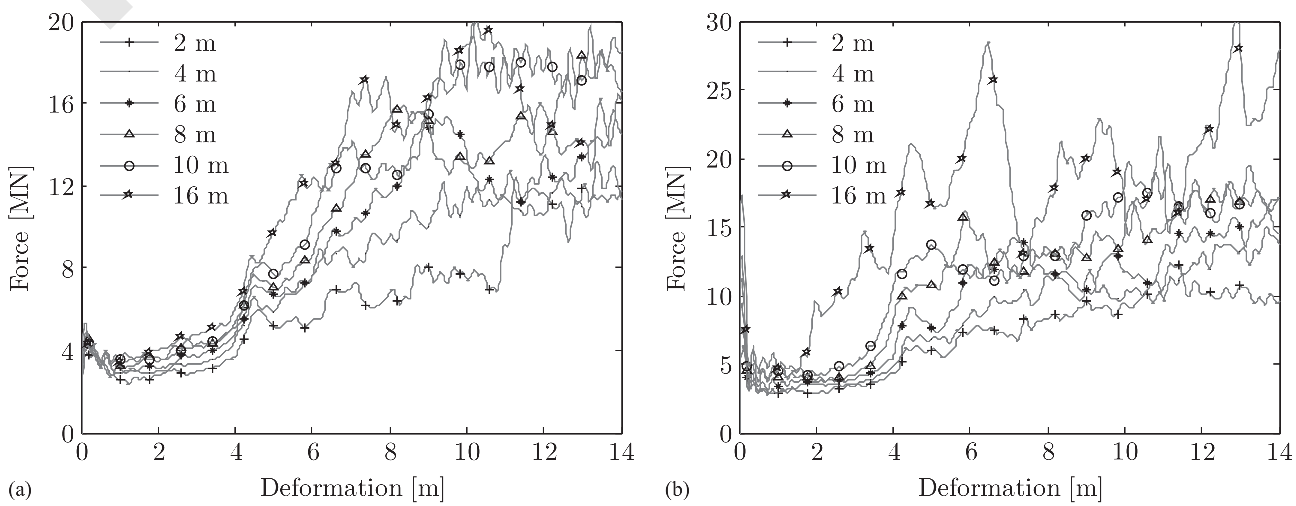

Fig. 10. Load deformation for cargo barge for centered impact against (a) round pier; and (b) flat pier

- Following the initial peak, the contact forces decrease or remain approximately constant up to a deformation of about 5 m. During this stage, the internal trusses in the bow and the hull buckle, whereas the barge body does not undergo considerable deformations [Fig. 8(b)].
- For deformations greater than 5 m, the contact forces undergo a sharp increase, to a level even greater than the initial peak, mainly owing to the contact of the pier with the barge body [Fig. 8(c)]. This effect is more pronounced for tanker barges, which include a steel structure that covers the payload (Fig. 4).
- It is observed that contact forces do not significantly change for deformations greater than 14 m (Fig. 11).

In contrast to the empirical force-deformation curves adopted in codes, such as AASHTO (2012), numerical results show that contact forces do not steadily increase with deformation. Hence, impact forces may be overestimated or underestimated for different pier geometries or collision energies.

Some of these trends are consistent with results previously reported by other authors (Consolazio et al. 2008; Harik et al. 2008). For example, Fig. 12 shows a comparison of the load-deformation curve for a Parana cargo and Jumbo hopper (Consolazio et al. 2008) barges impacting a flat pier, where the results are quite similar within the deformation range considered by previous studies.

However, the sharp increase in collision forces for deformations larger than 5 m was not identified in previous studies and may have a significant influence on the forces developed for high-energy collisions.

Typical FE results of centered impacts against flat and rounded piers are shown in Figs. 9 and 10. In these figures, FE results were smoothed for a simpler representation, filtering out sharp force variations at incremental deformations under 0.4 m.

Force-deformation relationships for corner impacts were also derived using the FE models. The collision forces obtained for corner impacts are similar to the centered impact results, with the exception of narrow piers, where the mean impact force is lower for corner impacts [Fig. 9(b) versus Fig. 13(a), and Fig. 10(a) versus Fig. 13(b)]. A conservative assumption would consider that an impact of two adjacent barges with a bridge pier occurs at the corner of both barges, as opposed to considering a centered collision of a single barge.

Oblique impacts against flat walls at different collision angles were also analyzed using the FE model. In these analyses, the same modeling scheme used for centered impacts was considered. However, for the full barge models, the lateral sides of the barges were prevented from moving along the direction perpendicular to the initial velocity to prevent barge rotation during the collision process (as expected for flotilla collisions).

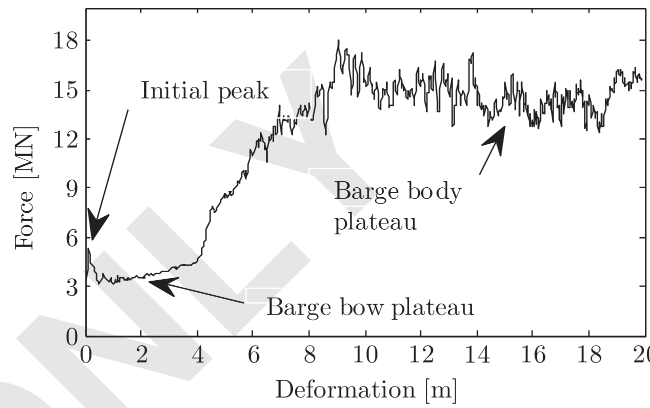

Fig. 11. Extended load-deformation result for centered impact of cargo barge against 8 m flat pier

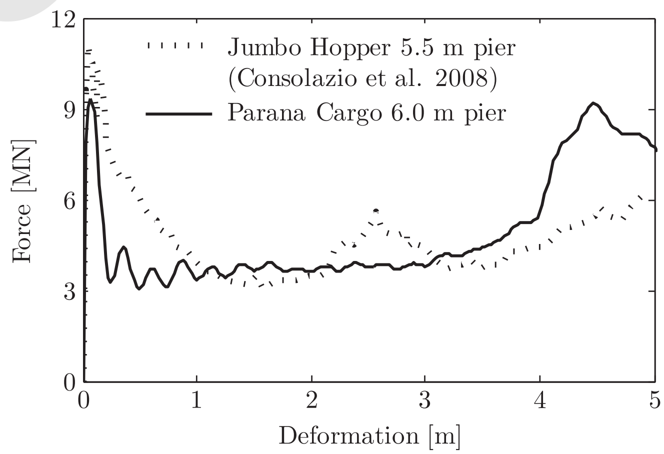

Fig. 12. Force versus deformation for Parana cargo barge and Jumbo hopper (data from Consolazio et al. 2008) against flat pier

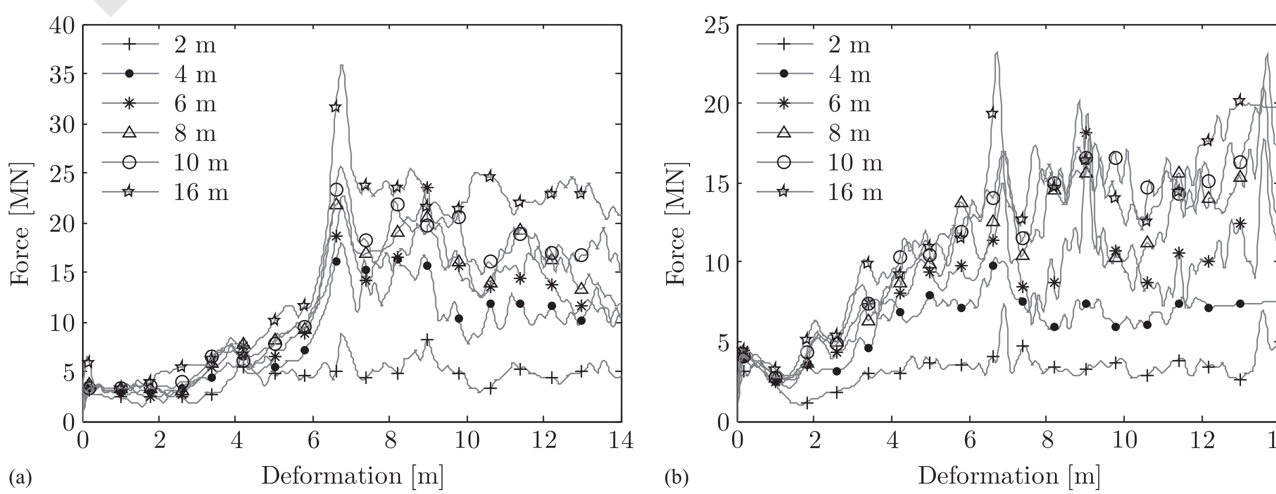

Fig. 13. Force versus deformation for corner impacts: (a) tanker barge against flat pier; (b) cargo barge against round pier

In the analysis using the partial-barge model, deformations were found to localize near the boundary section for oblique impacts [Fig. 14(a)]. This behavior is considered a fictitious consequence of the boundary condition of the partial model because this behavior was not observed for the full-barge FE models [Fig. 14(b)].

For the case of oblique impacts against flat walls, it was observed that there is a decrease in the collision forces for increasing impact angles with respect to a head-on collision (Fig. 15). The results herein presented consider the deformation measured along a normal direction with respect to the impacted wall.

Simplified Force-Deformation Relations

The FE model results for centered, corner, and oblique impacts were approximated by piecewise linear functions to make these results readily available for implementation in simplified analysis methods, as discussed further on in this paper. The force-deformation relations were defined using 10 points, fitted following the sequential quadratic programming method to minimize the quadratic residual. The following restrictions were imposed:

- First point is the force-deformation origin ($F = 0$; $\delta = 0$),
- Force magnitudes must be positive,
- Deformations are given in increasing order, and
- Last value of deformation equals to the maximum deformation reached in the analyses ($\delta = 14\,\mathrm{m}$).

A comparison of the force-deformation relationships considering the full FE model results and the piecewise linear approximation is shown in Fig. 16. The simplified relationships for centered, corner, and oblique impacts are summarized in the Appendix.

Simplified Analysis Methods

Full FE models for barge–bridge interaction analyses are not generally available for design because of the lack of detailed information on the barge structure and the time cost associated with the model definition and solution of the nonlinear problem. Hence,

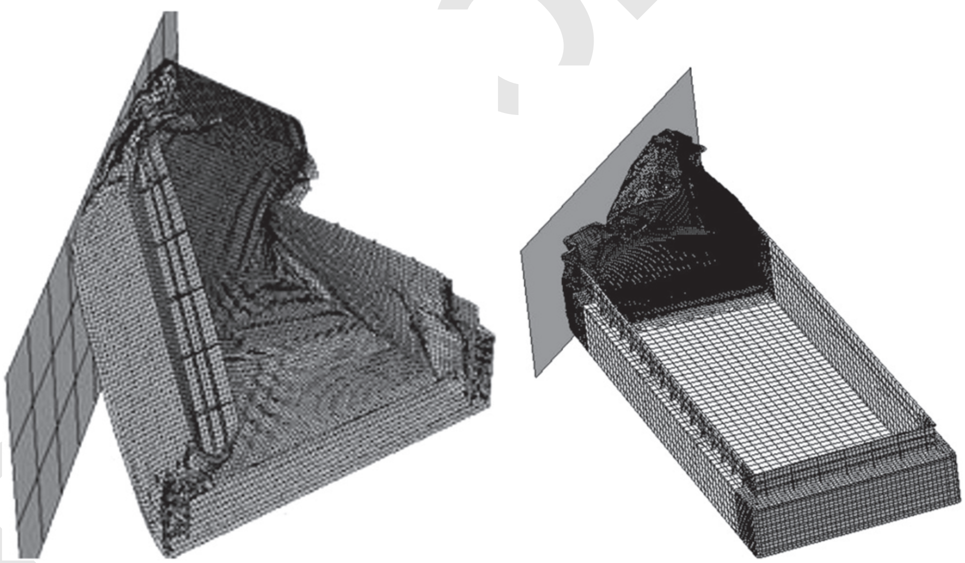

(a) (b)

Fig. 14. Behavior of partial-barge and full-barge models during oblique impacts against flat wall

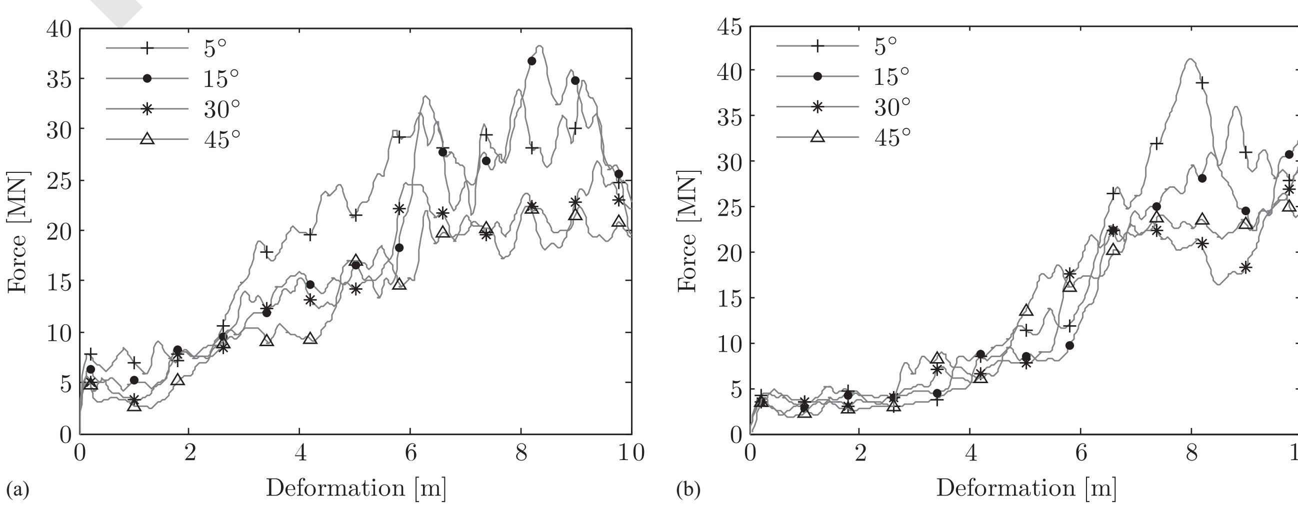

Fig. 15. Load deformation for oblique impacts against flat wall: (a) cargo barge; (b) tanker barge

simplified low-resolution analysis methods are warranted for design. This paper proposes simplified methods that include key aspects of the barge–bridge collision process.

Two simplified methods, which are able to represent symmetrical and oblique impacts, are presented and validated using full FE model results. These simplified methods consider the piecewise linear relationships described above to account for the structural behavior of the barges. Alternatively, a modification of a simplified procedure previously proposed by Consolazio et al. (2008) is presented to consider a more detailed force-deformation characterization of the barges applicable to high-energy collisions. These methods are applicable to different impact scenarios, as discussed in the following sections.

Simplified Coupled Model for Symmetric Impacts

Consolazio et al. (2008) proposed an analysis method, referred to as CVIA, in which barges are modeled as single masses connected to the bridge structure using a contact force. This model can be readily implemented in commercially available structural analysis software, such as *SAP2000*. This approach considers several aspects of the collision phenomenon, such as the dynamic response of the impacted structure, barge mass and speed (i.e., kinetic energy), and a piecewise linear force-deformation relationship for the barge structure.

A key assumption of this simplified modeling approach is that a barge column can be represented by a single mass. This assumption, however, does not introduce significant differences in results for symmetric impacts because kinetic energy is mainly dissipated by elastoplastic work in the front barge (e.g., Harik et al. 2008). For multicolumn barge flotillas, an equivalent procedure that can account for the influence of barge columns that do not come in contact with the bridge pier was proposed by Luperi and Pinto (2014).

In the proposed approach, the structural model is augmented with two additional degrees of freedom (DOF), representing interaction with the impacting barges. The first DOF, where the barge mass is assigned, is connected by a piecewise linear (i.e., nonlinear) element to a second DOF (link/support element with multilinear plastic behavior), which in turn is connected by a compression-only spring element to the impact point in the bridge structure (gap element). A schematic representation of this modeling approach is shown in Fig. 17. The stiffness of the compression-only spring is of an order of magnitude greater than the nonlinear element to avoid significantly affecting the results. In addition, a stabilizing mass is assigned to the second DOF.

A nonlinear direct time-integration scheme is considered for the analysis. Because an initial velocity cannot be assigned as an initial condition, two consecutive analysis stages need to be defined. The displacements and velocity of the nodes at the end of the first stage are used by the program as initial conditions for the second stage.

In the first stage, a force is applied to the barge mass, which is accelerated to the desired impact velocity at the end of this stage. The barge mass accelerates freely because an element is defined with a gap equal to the total free displacement needed for the mass to accelerate to the desired velocity.

The results obtained using this simplified analysis procedure are compared with results of a full FE model, where the impacted structure (bridge) is considered as rigid to assess the influence of the barge model only. The final configuration and load history for

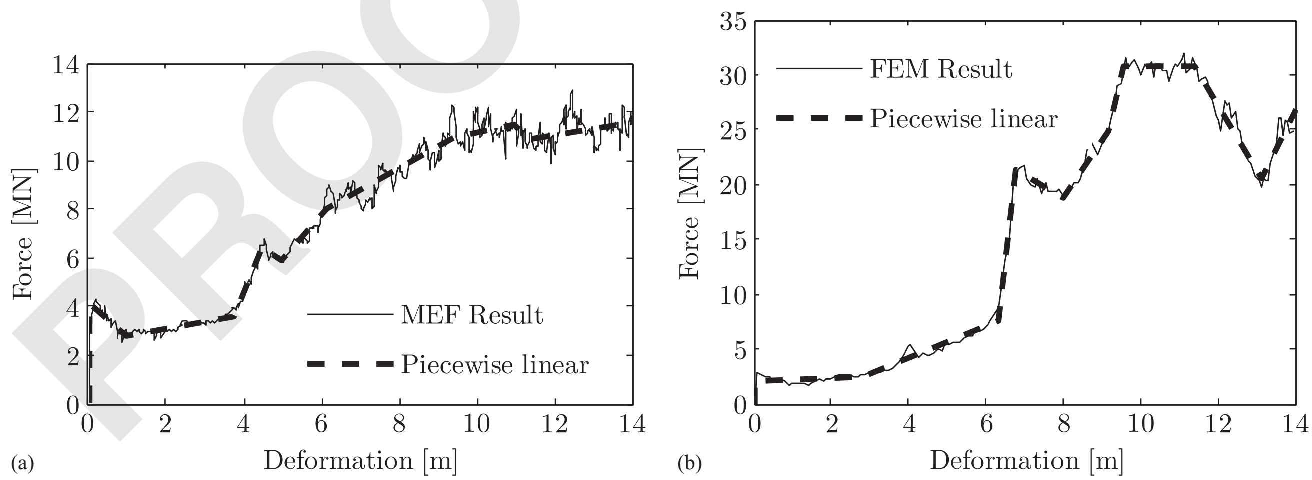

Fig. 16. Load deformation—FE model results versus piecewise linear approximation: (a) cargo barge against 4 m flat pier; (b) tanker barge against 10 m round pier

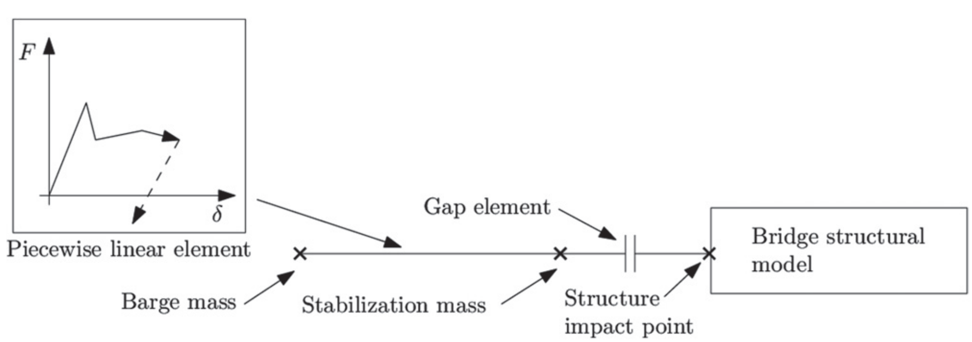

Fig. 17. Simplified model for symmetric impacts

a column of three cargo barges (2,900 t each) impacting at 5 m/s against a 6 m flat pier are shown in Figs. 20 and 21, respectively. It can be seen that there is a very good agreement between the full FE model and simplified model results. In this example, the maximum barge deformation obtained using the FE model analyses and simplified model is 12.05 and 12.17 m, respectively, whereas the dissipated energy is 96.0 and 95.9 MJ for each modeling approach.

Although this proposed modeling approach involves little extra effort on the bridge model for the collision analysis, it is able to accurately represent key aspects of the collision phenomenon, and yields force histories that do not substantially differ from full FE analyses, as shown in Fig. 21.

Applied Load History Method Modification for High-Energy Collisions

A simplified method, referred to as the AVIL, was proposed by Consolazio et al. (2008). In this method —applicable to symmetric impacts—a load history is derived using a set of design parameters (e.g., barge velocity and mass) and subsequently applied to the structure. This method is based on principles of conservation of energy and linear momentum and assumes an elastic-perfectly plastic behavior for the barge bow. This simplified method has been validated using the more elaborate CVIA (Consolazio et al. 2008). However, FE analyses for high-energy collisions indicate there is a significant force increase after a certain deformation at the barge bow. Thus, a modification to this method is herein proposed to account for the increase in crushing forces for high-energy collisions (i.e., large bow deformations).

To determine the crushing forces of the barge (controlled both by bow and body), as well as the deformation at which the transition of crushing forces occurs, the curves showing the variation of energy with deformation (obtained using the FE models) are approximated by bilinear relationships (Fig. 18).

On the basis of these results, the crushing forces at different deformation ranges, as well as the transition point, are derived as a function of pier size and shape. The approximations are summarized using the following linear equations:

$$T_P = A_d + B_d D$$

$$P_1 = A_{F1} + B_{F1} D$$

$$P_2 = A_{F2} + B_{F2} D$$

$$k_B = A_K + B_K D \quad (1)$$

where $T_P =$ transition point (deformation at which the crushing force increases) in meters; $D =$ pier width in meters; P_1 and $P_2 =$ barge bow and body-crushing loads, respectively; $k_B =$ barge stiffness; and A and $B =$ parameters summarized in Table 2.

The load history can thus be estimated using the AVIL method as proposed by Consolazio et al. (2008), where the trial crushing deformation of the barge for inelastic impacts (considering a unique crushing force) can be estimated using the following equations:

$$a_B = \frac{1}{2}\frac{m_B}{P_1} V_{BY}^2 \quad (2)$$

$$V_{BY} = \sqrt{V_{Bi}^2 - \frac{P_1^2}{k_S m_B}} \quad (3)$$

$$k_S = \left(\frac{1}{k_B} + \frac{1}{k_P}\right)^{-1} \quad (4)$$

where $a_B =$ trial barge-crushing deformation; $V_{BY} =$ barge velocity at beginning of yield; $V_{Bi} =$ initial barge velocity; $m_B =$ barge mass; P_1 barge-bow crushing force; $t =$ time until elastic rebound; $k_S =$ effective barge-pier-soil spring stiffness; and k_B and $k_P =$ barge and equivalent pier stiffnesses, respectively.

By comparing the trial crushing deformation with the transition point, it can be determined whether the load history can be obtained using the AVIL procedure, as proposed by Consolazio et al. (2008), considering a single initial crushing force. If the trial crushing deformation is greater than the transition point, then a double-yield load history is determined, where the yield loads represent the crushing forces controlled by the bow and body of the barge. This two-stage load history, herein referred to as

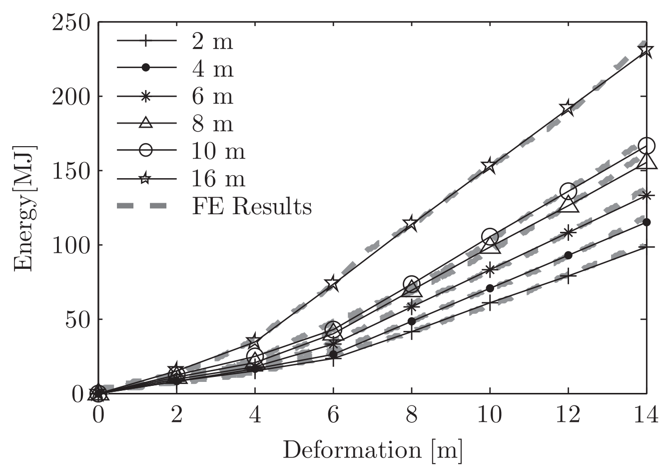

Fig. 18 Energy-deformation relationship for Parana cargo barge for centered impacts against flat pier 13

Table 2. Parameters for Transition Point and Barge Bow and Barge-Crushing Load

	Cargo barge				Tanker barge			
	Round pier		Flat pier		Round pier		Flat pier	
Parameters	*A*	*B*	*A*	*B*	*A*	*B*	*A*	*B*
t (m)	6.54	– 0.07	6.29	– 0.15	6.81	– 0.03	6.88	– 0.13
F1 (MN)	3.44	0.08	2.94	0.27	2.7	0.04	2.28	0.08
F2 (MN)	8.95	0.55	8.15	0.73	15.06	0.85	16.37	0.61
k_B (MN/m)	264	69	212	81	79	– 3	35	8

modified applied vessel impact load (MAVIL), is determined as follows:

1. First, the duration of the elastic loading is determined as proposed by Consolazio et al. (2008):

$$t_Y = \frac{\pi m_B}{2P_1}(V_{Bi} - V_{BY}) \tag{5}$$

2. Next, the duration of the plastic phase caused by yielding of the barge bow is estimated, as follows:

$$t_1 = m_B \frac{V_{BY} - \sqrt{V_{BY}{}^2 - 2P_1 T_P/m_B}}{P_1} \tag{6}$$

3. Then, the velocity at which the transition point is reached is calculated:

$$V_1 = V_{BY} - \frac{P_1 t_1}{m_B} \tag{7}$$

4. The duration of the plastic yielding at the barge body is determined as

$$t_2 = \frac{m_B V_1}{P_2} \tag{8}$$

5. Finally, the duration of the elastic unloading is obtained:

$$t_u = \frac{\pi}{2} \frac{m_B}{\sqrt{k_S m_B}} \tag{9}$$

On the basis of these parameters, the load history is obtained as shown in Fig. 19.

The load history obtained using the MAVIL method is compared against full FE model results and the simplified coupled method in Fig. 21. Although there are some differences, the MAVIL method can represent the main features of the impact history and the crushing force variation for high-energy collisions. The variation in crushing force would not have been represented by the original AVIL procedure (Consolazio et al. 2008) because it was originally developed for a lower deformation range. Hence, it is considered that the MAVIL method is a reasonable approximation for design in high-energy collisions.

Simplified Model for Oblique Impacts

Although not generally a controlling scenario in design, the analysis of oblique impacts may be warranted in different situations, e.g., collisions with a structure that has slanted sides to deflect impacting vessels, or an eccentric flotilla collision. One significant assumption for the analysis of symmetric impacts is that the position of barges is given by a single coordinate, which is an unrealistic assumption for oblique impacts. Moreover, other phenomena generally not considered in symmetric-impact models may need to be accounted for, such as failure of lashings, interaction among barges, and geometric interaction with piers.

For these situations, a simplified bidimensional analysis method was proposed by Luperi and Pinto (2014). In this approach, barge and pier are defined using meshes, consisting of a group of points that define their respective contours. The contacts between different elements of the model are detected on the basis of the contour meshes using a contact algorithm (Luperi and Pinto 2014). This algorithm determines which points of a particular barge mesh fall inside the contour defined by an adjacent barge or pier mesh. Hence, a contact zone, its normal direction, a contact overlap, and a relative tangent velocity are derived. On the basis of these parameters, the resulting contact forces within the barge tow are determined. The dynamic barge collision analysis is performed using a numerical integration scheme of the equations of motion of the full barge-structure system.

The force-deformation behavior of the barge bows and lashings are represented using nonlinear springs. Barges that do not directly impact the pier are considered to behave as linear elastic. This simplifying assumption is considered a reasonable approximation on the basis of full FE analyses of barge columns reported by Harik et al. (2008), where it is shown that energy dissipation is mainly caused by the plastic deformation of the impacting barge bow.

The flotilla model proposed by Luperi and Pinto (2014) can represent oblique impacts, model the behavior of lashings, and account for piecewise linear bow behavior and the dynamic response of the structure.

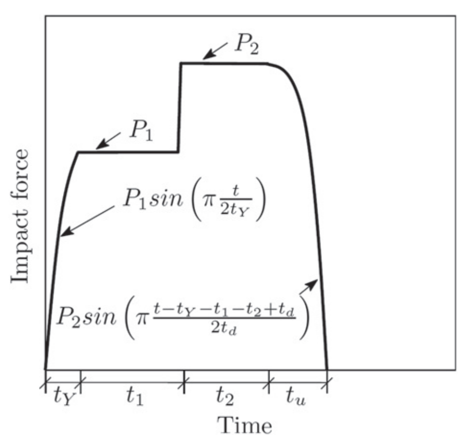

Fig. 19. Modified applied vessel impact load method

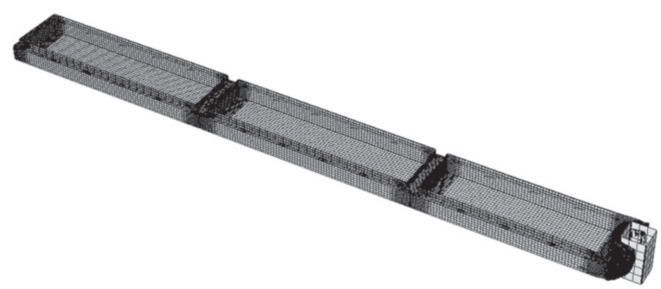

Fig. 20. Final configuration of a three-barge column impacting a 6 m flat pier at 5 m/s

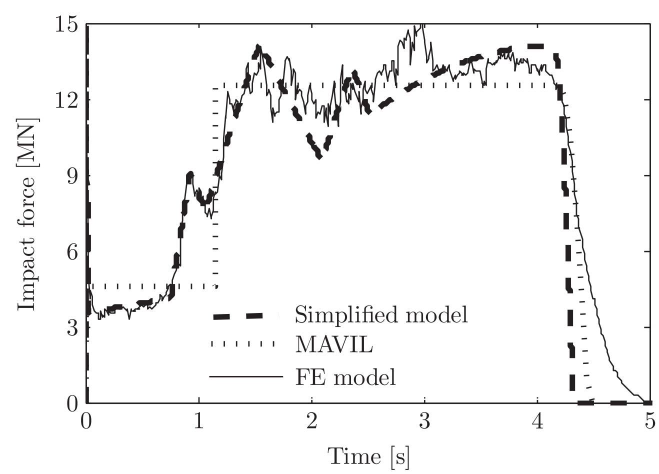

Fig. 21. Impact-force history of a barge column impacting a 6 m flat pier

14

The oblique force-deformation relationships for high-energy collisions herein presented can be readily incorporated in this bidimensional approach as piecewise linear relations. As an example of typical results, the contact-force history for an oblique impact (30°) of a 2×2 barge flotilla against a flat wall, with an initial velocity of 5 m/s is considered. The final configuration, load history, and evolution of energy are shown in Figs. 22–24. In this example, the first barge column impacts the flat wall, whereas the second barge column breaks away and later collides with the wall. The impact of both barge columns occurs simultaneously at $t = 1.9–2.2$ s after initial contact. During this time interval, a peak impact force caused by the contribution of both columns can be seen in the load history. Some discrepancies exist between the load histories evaluated using each method; however, the impulse delivered to the flat wall is 53.1 and 51.8 MN for the simplified two-dimensional (2D) approach and full FE models, respectively (a 2.5% difference). The evolution of energy is shown in Fig. 24, where the kinetic and dissipated energies through friction and plastic work are compared. The simplified 2D approach yields reasonable results, consistent with general engineering approximations, for oblique impacts of barge flotillas. The total time for the definition of the simplified 2D model and computation is a fraction of the time required for the full FE model setup. Therefore, it is considered that the simplified 2D model proposed by Luperi and Pinto (2014), including the force-deformation relationships for oblique impacts presented herein, is a useful technique for routine analysis of barge flotilla impacts, particularly for design.

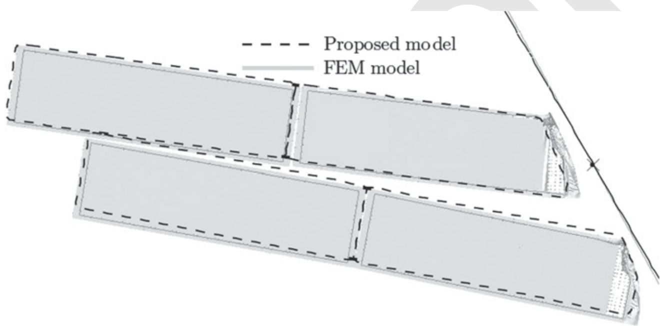

17 **Fig. 22.** Final configuration for oblique impact of a 2×2 barge flotilla against a flat wall

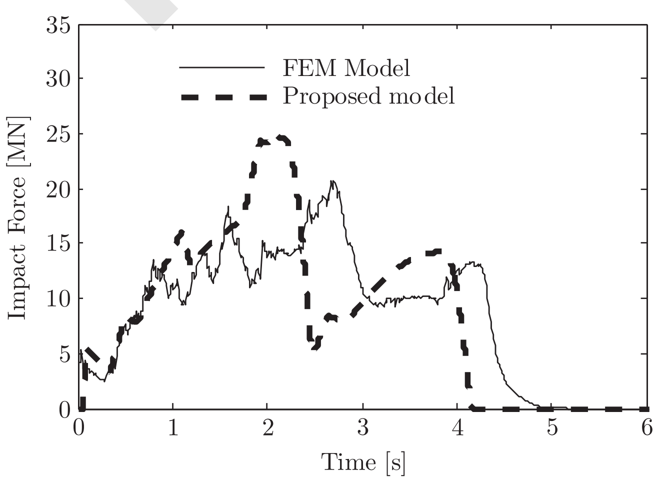

18 **Fig. 23.** Load history for oblique impact of a 2×2 barge flotilla against a flat wall

Conclusions

The structural behavior of Parana cargo and tanker barges was studied using high-resolution FE models. Several collision simulations, considering different shapes and sizes of impacted structures, were performed using the numerical models. Nonlinear force-deformation relationships were obtained for an extended range of bow deformation to better define the structural behavior of barges for high-energy collisions. It was found that the impact forces increase considerably for deformations greater than the length of the barge bow. Piecewise linear approximations of force-deformation relationships are given for centered, corner, and oblique impacts. These relationships can readily be incorporated in simplified analysis methods.

A simplified modeling approach for symmetric impacts is proposed for its implementation in commercially available structural analysis software. The proposed modeling approach is simple, but able to consider key features of the collision, such as structural response (particularly relevant for flexible protection structures), dynamic amplification, and nonlinear (i.e., piecewise linear) structural response of the barge. Piecewise linear relations are given for high-energy collisions, where the yield load increases for large deformations. This increase in yield load was not identified in previous studies by Consolazio et al. (2010a) and Harik et al. (2008).

The MAVIL method proposed in this paper is applicable to high-energy collisions and allows derivation of the impact-force history, which can later be applied to the structure. This proposed method can represent the crushing-force variation for high-energy collisions, where deformations exceed the range considered by previous studies.

The force-deformation relationships herein presented are also applied to the analysis of oblique impacts of barge flotilla. The proposed force deformations are implemented in a simplified 2D model presented in a previous paper (Luperi and Pinto 2014).

The results obtained using the proposed simplified approaches closely represent the results obtained using more elaborate (and time consuming) FE models.

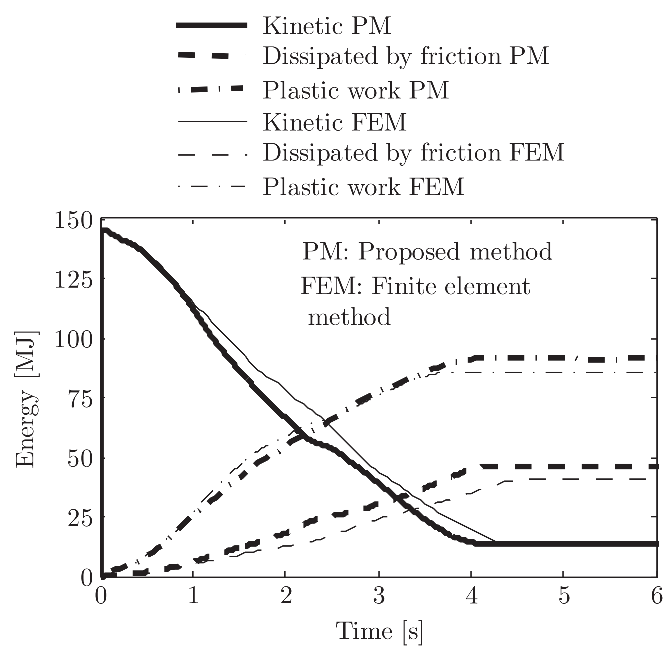

Fig. 24. Energy evolution for oblique impact of a 2×2 barge flotilla against a flat wall 15

Appendix. Simplified Force-Deformation Relations

Piecewise Linear Force-Deformation Relationship for Centered Impact of Parana Cargo Barge

Dimension (m)			Load-deformation relationships									
Round pier	2	*D*	0.01	0.33	0.93	3.92	4.56	4.89	10.92	11.29	12.61	14.00
		F	3.34	3.93	2.44	3.37	6.06	5.37	8.03	11.95	10.67	12.92
	4	*D*	0.03	0.98	3.75	4.48	4.96	6.15	9.44	11.00	11.28	14.00
		F	4.14	2.77	3.63	6.44	5.87	8.00	10.98	11.46	10.89	11.56
	6	*D*	0.02	1.15	3.86	4.51	5.29	8.15	9.38	10.43	12.67	14.00
		F	4.16	2.84	4.24	7.12	6.59	12.28	15.82	11.67	12.63	15.34
	8	*D*	0.01	0.90	3.89	4.42	5.40	8.36	9.51	10.53	13.54	14.00
		F	4.33	3.09	4.78	7.50	7.15	16.24	12.95	13.29	18.18	16.69
	10	*D*	0.02	1.17	3.94	4.52	5.40	6.93	7.47	8.66	9.22	14.00
		F	4.42	3.25	4.72	8.07	7.96	14.13	12.47	13.05	17.34	18.20
	16	*D*	0.02	0.47	3.67	5.72	6.27	7.32	8.37	10.51	11.97	14.00
		F	5.67	3.25	5.11	12.24	11.94	17.07	14.77	20.12	13.76	15.12
Flat pier	2	*D*	0.02	0.29	3.72	4.48	5.41	5.80	6.91	11.01	11.04	13.99
		F	7.50	2.90	3.47	6.30	5.52	7.46	7.37	10.09	11.44	9.36
	4	*D*	0.02	0.14	3.76	4.39	5.43	6.59	7.76	8.02	9.96	13.99
		F	12.79	3.10	3.83	6.89	6.85	9.60	9.72	11.82	9.83	14.48
	6	*D*	0.02	0.13	3.66	4.45	5.06	7.05	8.90	9.68	10.08	13.99
		F	16.55	3.56	4.09	9.08	7.53	14.20	9.56	13.22	11.38	16.55
	8	*D*	0.02	0.11	3.37	4.33	5.22	5.86	6.99	8.57	13.34	14.00
		F	21.43	4.30	4.06	10.53	10.72	15.34	11.69	12.91	18.35	14.23
	10	*D*	0.02	0.11	3.19	4.29	4.99	6.34	8.61	10.15	12.25	14.00
		F	26.32	4.75	4.63	12.27	13.26	11.09	13.64	18.57	16.36	17.05
	16	*D*	0.02	0.11	1.23	4.69	5.31	6.49	7.30	9.57	10.07	14.00
		F	31.94	7.33	3.82	19.21	15.54	28.29	13.70	22.92	15.46	26.90

Note: *D* = deformation (m); *F* = force (MN).

Piecewise Linear Force-Deformation Relationship for Corner Impact of Parana Cargo Barge

Dimension (m)			Load-deformation relationships									
Round pier	2	*D*	0.21	1.65	3.69	7.48	7.90	10.06	10.14	12.44	12.84	14.00
		F	3.77	0.95	3.06	4.36	3.02	3.68	2.86	3.70	2.54	5.85
	4	*D*	0.13	1.17	1.66	2.76	3.81	6.19	6.67	7.87	10.28	14.00
		F	4.07	2.24	3.36	3.13	6.95	7.46	10.06	6.45	6.56	7.94
	6	*D*	0.10	1.41	1.79	4.86	6.22	6.86	7.64	8.96	10.76	14.00
		F	4.20	1.90	3.60	9.11	9.07	13.60	6.01	12.58	7.73	13.18
	8	*D*	0.09	1.30	6.03	6.34	6.93	7.23	9.13	9.49	11.42	14.00
		F	4.21	2.61	12.60	9.36	17.08	11.66	16.78	9.35	13.31	16.71
	10	*D*	0.08	1.17	4.04	4.21	6.25	6.89	7.39	8.82	11.73	14.00
		F	4.21	2.68	8.92	10.64	12.65	16.73	10.64	17.09	13.51	20.55
	16	*D*	0.03	1.30	3.41	5.58	6.47	6.73	6.95	8.89	10.41	14.00
		F	4.30	2.92	9.16	11.13	14.48	24.27	13.37	16.57	12.36	22.78
Flat pier	2	*D*	0.02	0.78	1.72	2.93	3.21	4.61	6.40	6.94	7.01	14.00
		F	4.47	1.91	3.73	1.57	4.48	6.71	3.56	8.67	4.19	5.57
	4	*D*	0.02	0.51	4.15	4.61	6.04	6.74	7.07	8.92	10.38	14.00
		F	6.52	2.43	9.05	11.79	9.35	18.77	8.29	14.17	8.63	17.33
	6	*D*	0.02	0.53	3.04	5.41	6.19	6.58	7.54	9.17	11.26	14.00
		F	7.75	1.70	7.71	11.37	12.96	16.45	11.26	17.66	10.17	18.48
	8	*D*	0.02	0.56	4.86	5.47	5.93	7.62	8.62	9.17	10.30	14.00
		F	8.57	1.95	12.73	10.68	13.79	11.73	20.85	15.01	13.30	16.15
	10	*D*	0.02	0.58	3.28	3.55	4.07	6.85	7.63	8.54	10.34	14.00
		F	9.66	1.66	9.75	7.80	10.33	16.39	11.15	18.01	13.37	17.29
	16	*D*	0.02	0.35	2.88	3.86	4.17	6.67	7.40	7.89	11.43	14.00
		F	15.75	2.36	9.50	7.88	11.49	17.98	12.18	14.91	14.76	20.02

Note: *D* = deformation (m); *F* = force (MN).

Piecewise Linear Force-Deformation Relationship for Oblique Impact against Flat Wall of Parana Cargo Barge

Impact angle (degrees)		Flat wall									
5	*D*	0.06	2.40	3.04	6.43	6.92	9.31	9.79	12.01	12.34	14.00
	F	6.76	8.14	16.02	30.40	25.96	32.24	23.59	24.97	31.05	40.71
15	*D*	0.03	1.30	3.85	5.71	6.31	6.82	8.47	10.30	11.27	13.00
	F	5.42	4.72	15.24	14.80	34.54	21.24	37.44	19.48	21.06	34.06
30	*D*	0.03	1.20	1.84	2.34	4.03	4.30	5.61	5.85	8.45	11.00
	F	5.29	3.11	8.00	7.35	15.21	12.22	16.21	22.95	19.88	27.16
45	*D*	0.02	1.35	2.80	4.43	4.91	6.06	6.27	8.46	11.92	13.50
	F	4.17	2.44	10.09	9.56	17.66	15.22	19.72	20.56	18.95	25.08

Note: *D* = deformation (m); *F* = force (MN).

Piecewise Linear Force-Deformation Relationship for Centered Impact of Parana Tanker Barge

	Dimension (m)		Load-deformation relationships									
Round pier	2	*D*	0.06	2.73	4.02	6.38	6.81	8.76	9.31	11.43	11.63	14.00
		F	2.10	2.07	4.65	3.88	13.70	13.22	15.04	13.14	16.81	19.19
	4	*D*	0.04	2.37	4.67	6.36	6.80	7.50	8.10	10.96	12.78	14.00
		F	2.07	2.19	5.12	5.55	15.25	17.97	14.16	15.75	21.25	21.54
	6	*D*	0.01	3.30	3.98	6.37	6.78	9.21	10.02	12.22	13.23	14.00
		F	1.91	2.20	4.55	5.41	16.47	17.61	17.09	29.47	26.35	24.92
	8	*D*	0.11	1.27	6.00	6.39	6.64	10.00	11.06	11.96	12.85	14.00
		F	2.56	1.75	5.43	7.88	14.90	27.51	21.14	26.70	22.28	27.45
	10	*D*	0.05	2.84	6.35	6.75	8.03	9.16	9.59	11.42	13.14	14.00
		F	2.08	2.39	7.60	21.37	18.82	24.82	30.73	30.75	20.51	26.83
	16	*D*	0.18	0.20	1.52	3.19	6.28	6.72	8.33	8.87	13.20	14.00
		F	5.51	2.64	1.78	3.82	9.43	21.64	25.39	31.16	20.70	30.35
Flat pier	2	*D*	0.10	1.24	4.08	6.20	6.67	7.77	8.42	9.25	9.33	14.00
		F	2.23	1.08	3.12	4.21	13.32	14.49	13.04	15.04	14.16	13.96
	4	*D*	0.01	2.96	5.65	6.25	6.70	8.11	9.38	9.89	12.26	14.00
		F	1.97	1.96	4.85	6.88	17.57	15.33	20.79	17.34	22.48	23.34
	6	*D*	0.09	0.22	2.98	6.17	6.71	6.82	9.61	10.65	11.57	14.00
		F	4.93	1.51	2.72	6.38	26.47	15.75	26.10	22.17	24.05	24.22
	8	*D*	0.15	0.29	3.45	3.99	4.08	6.13	6.69	7.12	10.72	14.00
		F	3.38	2.01	3.44	6.80	3.72	7.96	31.37	18.58	25.16	21.68
	10	*D*	0.08	0.33	3.12	6.28	6.67	7.26	8.91	9.54	11.04	14.00
		F	8.73	1.94	3.65	11.52	36.74	18.08	25.97	18.99	21.97	24.24
	16	*D*	0.04	0.65	3.25	6.39	6.81	6.91	8.63	10.23	11.28	14.00
		F	8.51	2.18	2.26	18.74	73.40	37.35	23.61	26.30	16.67	23.36

Note: *D* = deformation (m); *F* = force (MN).

Piecewise Linear Force-Deformation Relationship for Corner Impact of Parana Tanker Barge

	Dimension (m)		Load-deformation relationships									
Round pier	2	*D*	0.08	0.68	1.24	3.78	4.09	6.52	6.79	8.71	11.35	14.00
		F	1.77	3.28	1.40	2.21	5.04	1.91	5.44	3.51	3.68	3.00
	4	*D*	0.04	0.59	2.23	4.16	5.45	7.14	7.71	10.56	11.03	14.00
		F	1.80	3.30	1.64	5.22	5.41	9.47	6.89	6.78	7.98	6.83
	6	*D*	0.01	0.44	3.27	4.08	6.39	6.70	8.74	10.27	12.45	14.00
		F	1.91	3.27	2.02	6.38	6.73	12.88	13.13	7.58	9.83	8.34
	8	*D*	0.05	0.53	1.01	3.47	3.95	5.98	6.99	10.65	10.79	14.00
		F	1.65	4.75	2.27	3.67	5.98	4.53	17.28	10.47	12.74	9.11
	10	*D*	0.36	1.18	3.35	3.96	5.13	6.23	6.71	8.20	8.76	14.00
		F	4.62	2.22	3.40	6.25	6.61	10.60	18.61	12.91	18.27	9.82
	16	*D*	0.17	1.50	2.05	3.48	3.96	5.66	7.25	11.00	13.23	14.00
		F	3.81	2.80	4.80	5.24	7.67	6.68	21.47	15.58	19.55	13.11

(*Continued.*)

	Dimension (m)		Load-deformation relationships									
Flat pier	2	*D*	0.14	1.66	1.78	2.99	4.08	5.88	6.72	9.08	10.12	14.00
		F	3.00	1.61	3.35	1.71	4.84	4.47	5.77	6.27	3.86	5.35
	4	*D*	0.10	0.87	2.18	4.15	5.72	6.61	9.09	9.28	11.32	14.00
		F	3.37	2.99	2.40	6.06	5.83	14.52	14.86	9.57	10.65	10.99
	6	*D*	0.03	0.26	2.51	3.81	5.37	6.68	9.26	10.27	11.17	14.00
		F	3.67	3.34	2.47	6.61	6.29	16.76	19.13	12.30	16.15	9.75
	8	*D*	0.01	2.81	3.94	4.43	6.06	6.45	8.94	10.40	11.33	14.00
		F	3.41	3.24	8.35	6.38	10.87	18.58	19.51	12.77	18.98	11.76
	10	*D*	0.09	2.25	6.02	6.70	7.62	8.08	9.75	10.36	11.16	14.00
		F	3.38	3.57	9.79	25.35	15.04	20.46	19.76	14.43	18.07	16.37
	16	*D*	0.08	0.39	4.28	6.20	6.74	7.13	8.62	9.67	10.17	14.00
		F	7.20	2.60	7.29	13.41	37.12	22.74	24.34	19.91	23.93	21.79

Note: *D* = deformation (m); *F* = force (MN).

Piecewise Linear Force-Deformation Relationship for Oblique Impact against Flat Wall of Parana Tanker Barge

Impact angle (degrees)		Flat wall									
5	*D*	0.15	1.18	1.26	3.34	4.85	5.76	8.07	8.43	11.87	14.00
	F	4.40	3.46	4.84	2.87	11.45	12.36	41.36	33.50	20.79	26.71
15	*D*	0.24	1.01	3.63	3.78	5.77	6.55	8.41	9.18	9.74	14.00
	F	4.64	2.98	4.98	8.58	8.33	21.39	30.41	22.00	30.77	19.52
30	*D*	0.08	1.36	2.38	3.38	5.51	5.78	7.28	8.68	10.43	14.00
	F	2.63	3.47	3.40	5.99	8.72	19.12	23.12	17.01	31.52	16.72
45	*D*	0.21	2.63	2.79	4.46	5.31	6.34	6.91	9.97	10.37	14.00
	F	2.77	2.81	8.28	6.38	17.62	16.96	22.21	24.45	21.01	29.97

Note: *D* = deformation (m); *F* = force (MN).

References

AASHTO. (2012). *AASHTO LRFD bridge design specifications*, Washington, DC.

Arroyo, J. R., and Ebeling, R. M. (2005). *Barge train maximum impact forces using limit states for the lashings between barges*, U.S. Army Engineer Research and Development Center, Washington, DC.

Boyer, H. F. (2002). *Atlas of stress-strain curves*, ASM, Metals Park, OH.

CARIA (Coosa-Alabama River Improvement Association). (2014). ⟨http://
16 www.caria.org/barges_tugboats.html⟩ (Dec. 2014).

CEN (European Committee for Standardization). (1991). "Actions on structures, part 1–7." *Eurocode 1*, Brussels, Belgium.

Consolazio, G. R., Davidson, M. T., and Getter, D. J. (2010a). "Vessel crushing and structural collapse relations for bridge design." *Rep. No. 2010/72908/74039*. Dept. of Civil and Coastal Engineering, Univ. of Florida, Gainesville, FL.

Consolazio, G. R., Davidson, M. T., and Getter, D. J. (2010b). "A static analysis method for barge-impact design of bridges with consideration of dynamic amplification." *Rep. No. 2010/68901*. Dept. of Civil and Coastal Engineering, Univ. of Florida, Gainesville, FL.

Consolazio, G. R., McVay, M. C., Cowan, D. R., Davidson, M. T., and Getter, D. J. (2008). "Development of improved bridge design provisions for barge impact loading." *Rep. No. 2008/51117*. Florida DOT, Univ. of Florida, Gainsville, FL.

Harik, I. E., Yuan, P., and Davidson, M. T. (2008). "Equivalent barge and flotilla impact forces on bridge piers." *Research Rep. KTC-08-12/SPR261-03-1F*, Kentucky Transportation Center, College of Engineering, Univ. of Kentucky, Lexington, KY.

Luperi, F. J., and Pinto, F. (2014). "Determination of impact-force history during multi column barge flotilla collisions against bridge piers." *J. Bridge Eng.*, 10.1061/(ASCE)BE.1943-5592.0000544, 04013011.

Meier-Dörnberg, K. E. (1983). "Ship collisions, safety zones, and loading assumptions for structures in inland waterways." *VDI-Berichte*, 496(1), 1–9.

Pinto, F., Prato, C. A., and Huerta, P. J. F. (2008). "Vessel collision protection for chaco corrientes bridge using energy absorbing drilled shafts." *Mecanica Computacional*, 387(27), 813–832.

SAP2000 [Computer software]. Berkeley, CA, Computers and Structures.

SIMULIA. (2010). *Abaqus* user's manual, SIMULIA, Providence, RI.

AUTHOR QUERIES

AUTHOR PLEASE ANSWER ALL QUERIES

Q: A_NEW! ASCE Open Access: Authors may choose to publish their papers through ASCE Open Access, making the paper freely available to all readers via the ASCE Library website. ASCE Open Access papers will be published under the Creative Commons—Attribution Only (CCBY) License. The fee for this service is $1750, and must be paid prior to publication. If you indicate Yes, you will receive a follow-up message with payment instructions. If you indicate No, your paper will be published in the typical subscribed-access section of the Journal.

Q: 1_AU: Please provide the ASCE Membership Grades for the authors who are members.

Q: 2_AU: Please provide an English translation for the author footnotes.

Q: 3_AU: Please provide the postal codes in both the affiliations.

Q: 4_AU: If Jumbo is a branded product, Please provide the manufacturer name and location details.

Q: 5_AU: The figures have not been cited sequentially in the text. Please renumber the figures so they are cited in numerical order in the text per journal style.

Q: 6_AU: For all Figs. 1-24, use parentheses, not brackets, around units: i.e., (m), (MN), (MPa), etc.

Q: 7_AU: Please confirm change of AASTHO (2012) to AASHTO (2012) as per the reference list.

Q: 8_AU: If Parana is a branded product, please provide the manufacturer name and location details.

Q: 9_AU: Please define SR.

Q: 10_AU: In Fig. 7a-b, “full-barge model” is hyphenated, as is “front-portion” model. Should “front-portion” be replaced with “partial-barge”?

Q: 11_AU: In Fig. 11, hyphenate “barge-body” plateau and “barge-bow” plateau.

Q: 12_AU: In Fig. 16b, replace “FEM Result” with “FE model result”

Q: 13_AU: In Fig. 18, replace “FE Results” with “FE model results” for consistency with Fig. 16

Q: 14_AU: In Fig. 19, “sin” should be in roman type.

Q: 15_AU: In Fig.24, “FEM” is referred to for the first time in the paper as “finite-element method”, whereas elsewhere in the paper it is called “FE model”. Please double check.

Q: 16_AU: Please provide article title and complete acces date details in reference (CARIA, 2014).

Q: 17_AU: In Fig. 22, replace “FEM model” with “FE model”

Q: 18_AU: In Fig. 23, replace “FEM Model” with “FE model”